Theor Chem Acc (2012) 131:1128
DOI 10.1007/s00214-012-1128-8

REGULAR ARTICLE

Density functional theory studies on the Diels–Alder reaction of [3]dendralene with C_{60}: an attractive approach for functionalization of fullerene

P. Ravinder · V. Subramanian

Received: 30 March 2011 / Accepted: 11 August 2011 / Published online: 31 March 2012

Abstract The Diels–Alder reaction between C_{60} and [3]dendralene has been carried out using density functional theory based Becke's three-parameter hybrid exchange functional and Lee–Yang–Parr correlation functional (B3LYP) method with 6−31G* basis set. The importance of dispersion corrections has been assessed by performing calculation at dispersion corrected B2PLYP-D/6–31G* level. The results reveal that the fullerene can be functionalized using [3]dendralenes. Several new types of adducts viz. mono (**1**), bis (**1**–**1**′ and **1**–**2**), tris (**1**–**1**′–**2** and **1**–**2**–**1**′), tetrakis (**1**–**1**′–**2**–**2**′), pentakis (**1**–**1**′–**2**–**2**′–**3**), and hexakis (**1**–**1**′–**2**–**2**′–**3**–**3**′) can be formed by the stepwise addition of [3]dendralene due to its multifarious reactive sites. Furthermore, it is observed that the **1**–**2** additions are thermodynamically and kinetically more feasible than the **1**–**1**′ ones. The geometrical distortion energy (E_{dis}) exhibits a linear relationship with the corresponding reaction barrier heights. The HOMO and LUMO energies of various reactants elicit that DA reaction is driven by normal electron demand. It is interesting to note from the energy decomposition analysis that although the steric effects dominate the addition reaction, the dispersion interaction plays a significant role in the stabilization of transition states. It is evident from the density of state and HOMO–LUMO gap (E_{gap}) that the functionalization of C_{60} by [3]dendralene marginally alters the conductivity.

Keywords Dendralene · Fullerene · Diels–Alder reaction · DFT · HOMO · LUMO · Activation energy · Reaction energy · Distortion energy

1 Introduction

Dendralenes are cross–conjugated acyclic polyenes which are highly reactive and tend to polymerize. Typically, [3]dendralene is a very volatile solid that dimerizes quickly [1]. The higher homologues are crystalline and stable compounds when masked [2–4]. Although, they are more sensitive and polymerize in solution, they are stable enough to have been fully characterized by standard spectroscopic and analytical tools [5, 6]. Further, absorption maximum of these molecules is similar to that of 1,3–butadienes. The DA reactivity of [n]dendralenes is multifaceted [7–9]. Dendralenes are very useful building blocks for the synthesis of extended ring systems using DA addition reactions [10–13]. A variety of synthetic protocols for the formation of mono adducts are available [10–13]. [n]dendralene provides means for the straightforward synthesis of bis and tris adducts. Further, it has been shown that for DA addition using [n]dendralene dienophile does not have to be identical in the various stages of the reaction [8].

In natural science, fullerene (C_{60}) is a fascinating molecule. Owing to its spherical structure of regularly arranged unsaturated carbon centers, it is functionalizable in three dimensions [14–23]. Specifically, C_{60} possesses only one type of carbon atom and two types of C–C bonds: 30 bonds

Dedicated to Professor Eluvathingal Jemmis and published as part of the special collection of articles celebrating his 60th birthday.

Electronic supplementary material The online version of this article (doi:10.1007/s00214-012-1128-8) contains supplementary material, which is available to authorized users.

P. Ravinder · V. Subramanian (✉)
Chemical Laboratory, CSIR-Central Leather Research Institute, Council of Scientific and Industrial Research, Adyar 600020, Chennai, India
e-mail: subuchem@hotmail.com; subbu@clri.res.in

at the 6–6 ring fusions and 60 bonds at the 6–5 ring fusions. Amongst, various approaches used to functionalize C_{60}, DA and 1,3-dipolar cycloadditions are the most preferred strategies. Evidences from different studies show that C_{60} acts as a powerful dienophile in DA addition due to its electron withdrawing nature [24–30].

Several experimental and theoretical studies have been carried out on the DA reaction of C_{60} with various dienes [17–23, 31–36]. Krautler et al. have explored the multiple DA reaction between C_{60} and 2,3-dimethyl-1,3-butadiene [31]. They have identified the highly symmetric sixfold cycloaddition (hexakisadduct) product of fullerene [31]. The yield was found to be $\sim$26% [31]. The product results from the sixfold DA reaction of diene at the six symmetry equivalent 6–6 bonds located between the six-membered rings of fullerene. Thus, the extraordinary regiocontrol observed in the multiple DA reaction has been addressed by several researchers [31–36]. In the subsequent work, the reaction between C_{60} and anthracene as well as with other dienes was probed [32]. Hirsch and coworkers have also made several important contributions to the addition reaction of C_{60} [33–35]. Overall, previous experimental studies have indicated that in DA reactions the diene shows a clear preference to attack the 6–6 ring fusions of the fullerene core over the 6–5 ring fusions [31–36].

Previous pioneering theoretical calculations on fullerene provided interesting clues to the reactivity trends in C_{60} [37, 38]. Attempts have been made to unravel the origin of regiospecificity of DA reaction of C_{60}. Geerlings and coworkers have made significant contributions to the understanding of DA reaction of C_{60} and with various dienes [39, 40]. It is noteworthy to mention here that they have shown that the reactions are concerted in nature and proceed through a transition state possessing a considerable net aromaticity [39, 40]. Similarly, Sola and coworkers have made seminal contributions to the understanding of DA addition of C_{60} with dienes [41–50]. They have analyzed the regioselectivity of successive 1,3-butadiene DA cycloadditions to C_{60} [49]. In that study, the nine unique possible reaction pathways leading to the experimentally observed T_h-symmetric hexakisadduct have been investigated [49]. The enthalpy barrier for the cycloaddition changes from 16.2 kcal/mol in the formation of the monoadduct to 17.8 kcal/mol for the hexakisadduct and increases slightly with successive attacks [49]. Therefore, the reaction barrier height increases linearly [49].

The versatility of DA reaction of [3]dendralene offers an attractive means for the functionalization of C_{60}. However, to the best of our knowledge such a study has not been reported. Thus, an attempt has been made in this investigation to explore the DA reaction between [3]dendralene and C_{60}.

2 Computational details

Previous studies have shown that B3LYP method predicts the DA reactions in good agreement with experimental results [51–53]. Since optimization of transition state geometry involving C_{60} using large basis set is computationally demanding, efforts were devoted to select suitable basis set by modeling the DA reaction between the fragments of C_{60} and various dienes. The different diene and dienophile combinations are as follows: [3]dendralene-ethylene, [3]dendralene-5-methylidenecyclopenta-1,3-diene, [3]dendralene-benzene, [3]dendralene-cyclopenta[*fg*]acenaphthylene, and [3]dendralene-corannulene. It is found from the previous studies that corannulene behaves similar to C_{60} in Diels–Alder cycloaddition [54]. In the case of model reactions, the geometries of the all the reactants, TSs, and products were optimized using B3LYP [55, 56] method employing 6−31G*, 6−311+G*, and 6−311++G** basis sets without any geometrical constrains. The results are presented in Supplementary information. It can be seen that B3LYP/6–31G* is sufficient to model DA reaction between C_{60} and [3]dendralene. Hence, the geometries of the reactants, TSs, and products in the DA reaction between [3]dendralene and C_{60} were optimized without any geometrical constrains using B3LYP/6−31G* method. Recently, Sola et al. have shown that inclusion of dispersion effects is important to obtain results close to the experimental values [50]. Therefore, to include the dispersion energy contributions, total energies of the reactants, TSs, and products were calculated using (Grimme's empirical dispersion correction (DFT-D) was used in combination with the B2PLYP functionals (referred to as B2PLYP-D)) B2PLYPD/6–31G*//B3LYP/6–31G* level of theory [57, 58].

The consecutive addition of six [3]dendralenes with C_{60} were considered in the present study. The TSs were characterized by the single imaginary frequency criterion. The reactions considered in this study were assumed to follow the concerted mechanism. The energetics of the reaction during different stages of addition, geometrical distortion in TSs, thermodynamics and of kinetics parameters were derived from the calculations. To quantify the stability of various TSs, the global hardness was calculated. The total distortion energies (E_{dis}) of TSs were calculated from the distortion energies of dienes (E_{dis}(diene)) and dienophiles (E_{dis}(dienophile)) using the equation given below.

$$E_{dis} = E_{dis}(\text{diene}) + E_{dis}(\text{dienophile})$$

(E_{dis}(diene) and E_{dis}(dienophile) are distortion energies of diene and dienphile, respectively).[1]

The thermodynamic parameters were calculated in gas phase at 298.15 K temperature and 1 atm pressure. All the calculations were carried out with the help of GAUSSIAN 03 [59] suite of program. To unravel the different factors contributing to the stabilization of TS, energy decomposition analysis was carried out for the various TSs using BLYP-D/DZP method employing ADF program package [60–64].

3 Models

3.1 Various pathways for [3]dendralene addition to C_{60}

Sola and coworkers have clearly analyzed the different possibilities for the diene addition to C_{60} [49]. According to their study, diene can be added to C_{60} in nine different ways [49]. The various dienophile bonds of C_{60} considered in the present investigation for the DA addition with [3]dendralene are defined in Scheme 1. Since the reaction between C_{60} and [3]dendralene are computationaly expensive, various pathways for *bis* and *tris* adducts are only considered. For tetra, penta, and hexa additions, only one pathway was considered.

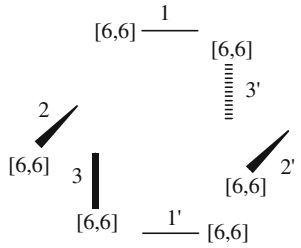

Reaction considered in the study

1: 1 → 1-1' → 1-1'-2 → 1-1'-2-2'

→ 1-1'-2-2'-3 → 1-1'-2-2'-3-3'

2: 1 → 1-2 → 1-2-1' → 1-2-1'-2'

→ 1-2-1'-2'-3 → 1-2-1'-2'-3-3'

Scheme 1 Schematic representation of the complete series of dienophile bonds involved in the reaction between [3]dendralene and C_{60}

[1] The distortion energies of diene and dienophile are defined as the energy difference between the corresponding geometries in transition state and isolated molecules. that is, E_{dis}(diene) = E_{dis} (diene in TS) − E (isolated diene) and E_{dis} (dienophile) = E_{dis} (dienophile in TS) − E_{dis} (isolated dienophile).

4 Results and discussion: DA reaction between [3]dendralene and C_{60}

4.1 Nomenclature and geometry

Broadly, the bonds in C_{60} are classified as [6,6] and [6,5] types depending on the neighborhood geometry. As shown in Scheme 1, the adducts obtained from DA addition of [3]dendralene with C_{60} are described based on the position of dienophile bond involved in the reaction. The position of the [6,6] bonds in C_{60} is represented as 1, 1′, 2, 2′, 3, and 3′. Adopting the nomenclature of Sola and coworkers [49], the mono adduct formed due to the diene addition at the position 1 is denoted as 1, and the corresponding TS is represented as $\mathbf{TS_1}$. Similarly, the product obtained upon subsequent addition of diene to the mono adduct (**1**) is represented as **1–1′** and the respective TS is designated as $\mathbf{TS_{1–1'}}$. The same nomenclature has been used throughout the remaining part of the text. In this work, structures and energy profiles of single mono adducts (**1**), two bis adducts (**1–1′** and **1–2**), two tris adducts (**1–1′–2** and **1–2–1′**), one tetrakis adduct (**1–1′–2–2′**), one pentakis adduct (**1–1′–2–2′–3**), and one hexakis adduct (**1–1′–2–2′–3–3′**) have been considered. As mentioned earlier, other possible adducts have not been considered due to the computational demand.

The optimized geometries of various TSs obtained for the reactions **1→1–1′→1–1′–2→1–1′–2–2′→1–1′–2–2′–3→1–1′–2–2′–3–3′** are depicted in Fig. 1 along with important bond distances. Geometrical parameters clearly reveal that the reactions follow the asynchronic path in all the stages. It can be found that the difference between newly forming bonds are 0.759, 0.841, 0.746, 0.437, 0.779, and 0.794 Å, respectively. Further, the reaction **1→1–2→1–2–1′** is also studied. Corresponding TSs (i.e., $\mathbf{TS_{1–2}}$ and $\mathbf{TS_{1–2–1'}}$) are given in Fig. 2 along with important geometrical parameters. It can be seen that the reaction along this reaction path leads to the formation of asynchronous product. Calculated *asynchronicity* values for the both stages are 0.683 and 0.773 Å, respectively.

Further, examination of the geometrical parameters of reactants and products discloses that C–C bonds in the neighborhood of the addition site in the C_{60} undergo considerable changes. Various bonds present in the neighborhood of addition site presented in Scheme 2. The geometrical parameters of these bonds are given in Table 1. The variations in C–C bond distance clearly provide information about the changes in the bond order and π-electron distribution. Moreover, the [6,5] bond distances are significantly larger than the [6,6] bonds in all the TSs. Specifically, the C–C bonds in the products undergo maximum elongation. These distances range from 1.61 to 1.62 Å for the reactions. The changes in the geometrical parameters of the

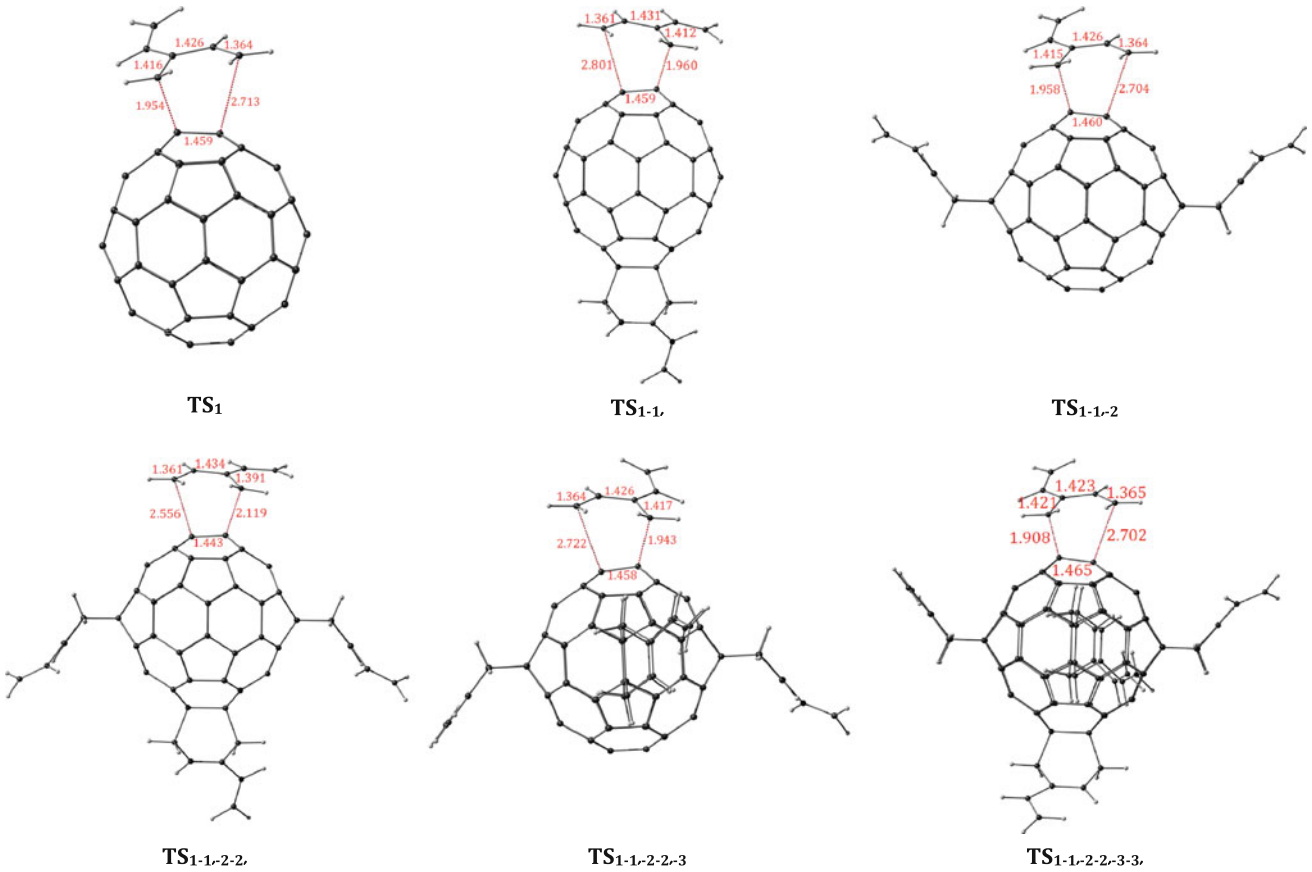

Fig. 1 Optimized geometries of TSs during various stages of the reaction between [3]dendralenes and C_{60} at B3LYP/6–31G* level (**1→1–1′→1–1′–2→1–1′–2–2′→1–1′–2–2′–3→1–1′–2–2′–3–3′**)

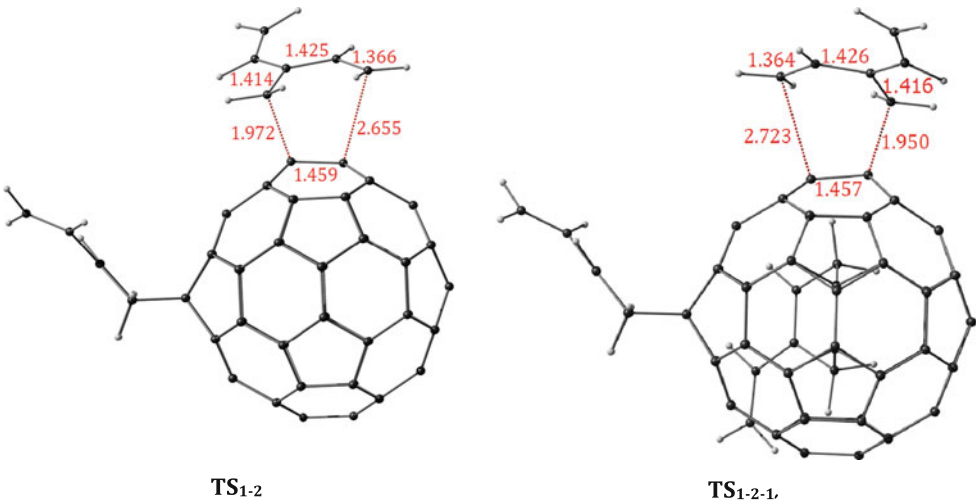

Fig. 2 Optimized geometries of TSs for **1→1–2→1–2–1′** reaction path way at B3LYP/6–31G* level

$TS_{1–2}$ and **$TS_{1–2–1'}$** are also similar to the above-mentioned trend. The elongation in bond lengths clearly reveals the transformation of unsaturated double bond to saturated single bond in the product formation. Further, the neighborhood bonds in the products retain the trend as observed in TSs. It can be seen from the results that the dihedral angles of dienophile undergo significant changes during various stages of reaction and hence associated alterations in the π-electron distribution.

4.2 Energetics and MESP

The calculated gas phase activation energy ($\Delta E^{\ddagger}$), activation free energy ($\Delta G^{\ddagger}$), reaction energy (ΔE_r), and reaction

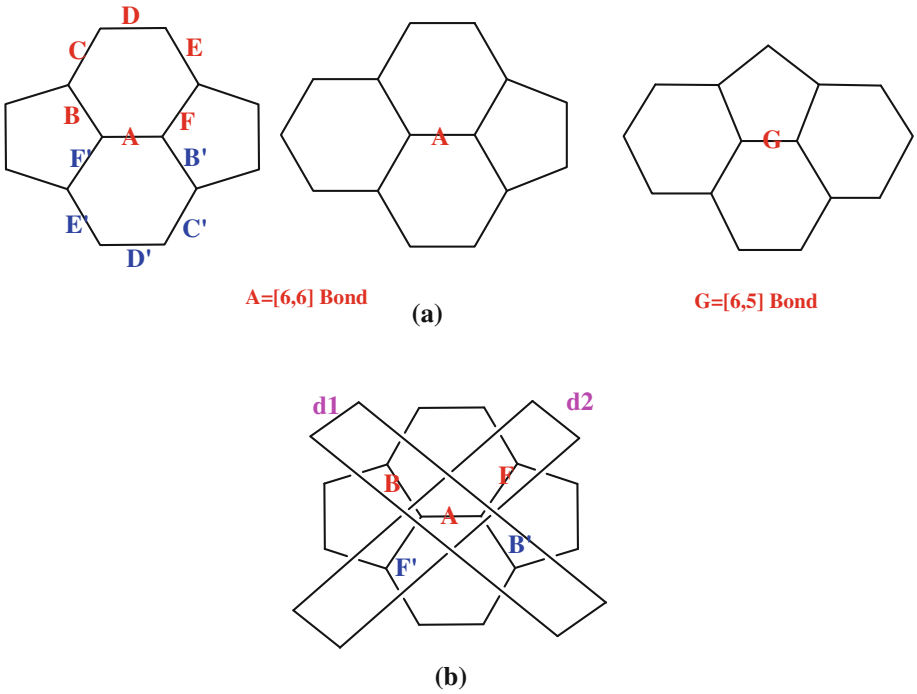

Scheme 2 **a** Definition of [6,6] and [6,5] type of bonds in C_{60} and important near neighborhood bonds of dienophile and **b** definition of dihedral angle

Table 1 Geometrical parameters in the near neighborhood of C_{60} in TSs and products

System	[6,6] A	[6,5] B	[6,6] C	[6,5] D	[6,6] E	[6,5] F	[6,5] B′	[6,6] C′	[6,5] D′	[6,6] E′	[6,5] F′	d1	d2
C_{60}	1.400	1.450	1.400	1.450	1.400	1.450	1.450	1.400	1.450	1.400	1.450	138.21	138.25
1	1.611	1.540	1.376	1.480	1.376	1.540	1.538	1.377	1.481	1.377	1.539	113.17	113.20
1–1′	1.612	1.540	1.377	1.481	1.377	1.541	1.539	1.378	1.482	1.378	1.538	113.16	113.19
1–1′–2	1.613	1.538	1.380	1.476	1.380	1.537	1.535	1.381	1.477	1.381	1.536	113.33	113.37
1–1′–2–2′	1.616	1.537	1.380	1.477	1.380	1.538	1.536	1.381	1.477	1.381	1.536	113.43	113.38
1–1′–2–2′–3	1.609	1.538	1.385	1.474	1.384	1.538	1.536	1.385	1.475	1.386	1.536	113.12	113.15
1–1′–2–2′–3–3′	1.610	1.535	1.385	1.475	1.385	1.536	1.538	1.385	1.474	1.385	1.537	113.24	113.24
$\mathbf{TS_1}$	1.459	1.503	1.386	1.466	1.392	1.455	1.454	1.394	1.464	1.386	1.503	128.33	128.48
$\mathbf{TS_{1–1'}}$	1.459	1.450	1.396	1.465	1.388	1.501	1.503	1.388	1.465	1.395	1.453	129.05	128.99
$\mathbf{TS_{1–1'–2}}$	1.460	1.500	1.390	1.462	1.396	1.453	1.453	1.398	1.460	1.391	1.501	129.01	129.16
$\mathbf{TS_{1–1'–2–2'}}$	1.443	1.463	1.393	1.469	1.388	1.490	1.490	1.389	1.467	1.393	1.464	130.26	130.07
$\mathbf{TS_{1–1'–2–2'–3}}$	1.458	1.452	1.400	1.464	1.393	1.501	1.502	1.394	1.462	1.401	1.453	128.99	128.72
$\mathbf{TS_{1–1'–2–2'–3–3'}}$	1.465	1.503	1.394	1.464	1.400	1.451	1.452	1.401	1.462	1.394	1.503	128.35	128.71
Other additions (bis and tris only)													
1–2	1.609	1.540	1.382	1.472	1.382	1.541	1.539	1.377	1.482	1.377	1.539	113.08	112.98
1–2–1′	1.610	1.538	1.386	1.471	1.382	1.541	1.539	1.378	1.479	1.380	1.537	113.24	112.97
$\mathbf{TS_{1–2}}$	1.459	1.500	1.390	1.463	1.393	1.457	1.457	1.395	1.461	1.390	1.500	128.31	128.57
$\mathbf{TS_{1–2–1'}}$	1.457	1.503	1.387	1.464	1.397	1.452	1.453	1.402	1.459	1.391	1.505	128.76	128.68

[6,6], [6,5] bond type, d1, and d2 dihedral angles are defined in Scheme 2

enthalpy (ΔH_r) are shown in Table 2. The extent of feasibility of the reaction is clearly evident from the $\Delta E^{\ddagger}$ and $\Delta G^{\ddagger}$ values. The ΔE_r and ΔH_r values indicate the stability of the various adducts. It is interesting to find that the barrier heights in the case of [3]dendralene with C_{60} increases linearly from $\mathbf{TS_1}$ to $\mathbf{TS_{1–1'–2–2'}}$. The B3LYP/6–31G* calculated values are 17.46, 18.08, 20.13, and 21.31 kcal/mol, respectively. The same values obtained using B2PLYP-D/6–31G* are 19.07, 19.44, 21.40, and 20.15 kcal/mol, respectively. The alteration in the activation energy with the level of theory may be attributed due to the inclusion of dispersion interaction in

Table 2 The energetics of various reactions

TSs	$\Delta E^{\ddagger}$	$\Delta G^{\ddagger}$	Adduct	ΔE_r	ΔH_r
$\mathbf{TS_1}$	17.46 (19.07)	31.25	**1**	−20.73 (−31.55)	−17.92
$\mathbf{TS_{1–1'}}$	18.08 (19.44)	31.85	**1–1′**	−21.35 (−32.40)	−18.45
$\mathbf{TS_{1–1'–2}}$	20.13 (21.40)	33.67	**1–1′–2**	−17.48 (−28.55)	−14.83
$\mathbf{TS_{1–1'–2–2'}}$	21.31 (20.15)	–	**1–1′–2–2′**	−19.21 (−30.23)	−16.40
$\mathbf{TS_{1–1'–2–2'–3}}$	18.93 (20.18)	32.40	**1–1′–2–2′–3**	−18.49 (−29.98)	−15.87
$\mathbf{TS_{1–1'–2–2'–3–3'}}$	19.97 (21.31)	33.94	**1–1′–2–2′–3–3′**	−16.03 (−27.72)	−13.35
$\mathbf{TS_{1–2}}$	17.76 (18.93)	31.75	**1–2**	−20.27 (−31.20)	−17.48
$\mathbf{TS_{1–2–1'}}$	15.47 (17.11)	29.59	**1–2–1′**	−22.51 (−33.44)	−19.60

The values given in parenthesis are calculated using B2PLYP-D/6–31G*//B3LYP/6–31G*, and the energies are in kcal/mol

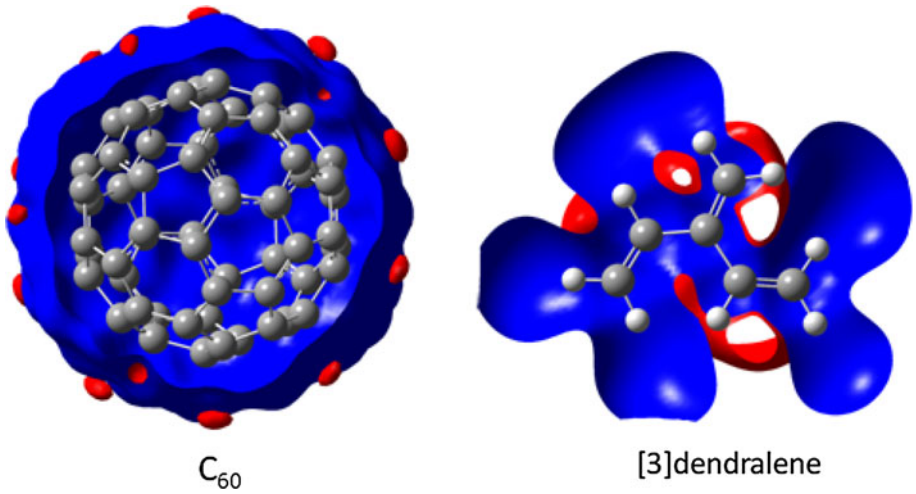

Fig. 3 Molecular electrostatic potential isosurfaces of reactants (0.004 a.u)

the calculations. It can be seen the $\mathbf{TS_{1–1'–2–2'–3}}$ and $\mathbf{TS_{1–1'–2–2'–3–3'}}$ barrier heights are comparatively smaller than $\mathbf{TS_{1–1'–2–2'}}$. Further, the $\Delta E^{\ddagger}$ values obtained for $\mathbf{TS_{1–2}}$ and $\mathbf{TS_{1–2–1'}}$ are 17.76 and 15.47 kcal/mol, respectively. These values are smaller when compared with the $\mathbf{TS_{1–1'}}$ and $\mathbf{TS_{1–1'–2}}$. It is noteworthy to observe that the $\Delta E^{\ddagger}$ values obtained for $\mathbf{TS_{1–1'}}$ and $\mathbf{TS_{1–2}}$ are in good agreement with the results of Hirsch and coworkers [33]. Furthermore, it can be seen that the trend in the $\Delta G^{\ddagger}$ of the reaction is similar to that of $\Delta E^{\ddagger}$.

The reaction enthalpy (ΔH_r) is calculated for all the reactions. Results indicate that the reactions considered in the study are exothermic in nature. The ΔE_r values calculated for the reaction clearly demonstrates the thermodynamic stability of the various adduct obtained during the reaction. Bis adduct **1–1′** and tris adduct **1–2–1′** are thermodynamically stable in the respective category. The calculated ΔE_r values for these adducts are −20.27 and −22.51 kcal/mol, respectively. The observed trend in the thermodynamics and kinetic parameters may be attributed to the changes in the symmetry of the π-cloud of the C_{60} and the secondary interaction of the [3]dendralene with the larger dienophile system.

To quantify the changes in the π-electron density, the molecular electrostatic potentials (MESPs) of the various systems were obtained from the calculation. The MESP topographical features of the structural motifs of C_{60} have been reported by Gadre and Jemmis as early as in 1996 [65]. They have shown that ethylene, [5]radialene, and corannulene are predicted to be the structural motifs of C_{60}. Further, their study revealed that benzene does not fit into this framework structure [65]. The calculated MESP isosurfaces of C_{60} and [3]dendralene are presented in Fig. 3. The MESP isosurfaces of all reactants, TSs, and products for reaction of C_{60} with [3]dendralene are displayed in supplementary information. The variations in the MESP

Table 3 The calculated distortion energies of various systems

TSs	E^{a}_{dis} (eV)	E^{b}_{dis} (eV)
$\mathbf{TS_1}$	0.59	0.278
$\mathbf{TS_{1–1'}}$	0.627	0.309
$\mathbf{TS_{1–1'–2}}$	0.589	0.436
$\mathbf{TS_{1–1'–2–2'}}$	0.503	0.291
$\mathbf{TS_{1–1'–2–2'–3}}$	0.61	0.475
$\mathbf{TS_{1–1'–2–2'–3–3'}}$	0.667	2.672
$\mathbf{TS_{1–2}}$	0.602	0.151
$\mathbf{TS_{1–2–1'}}$	0.594	0.237

[a] E_{dis} = diene

[b] E_{dis} = dienophile distortion energies

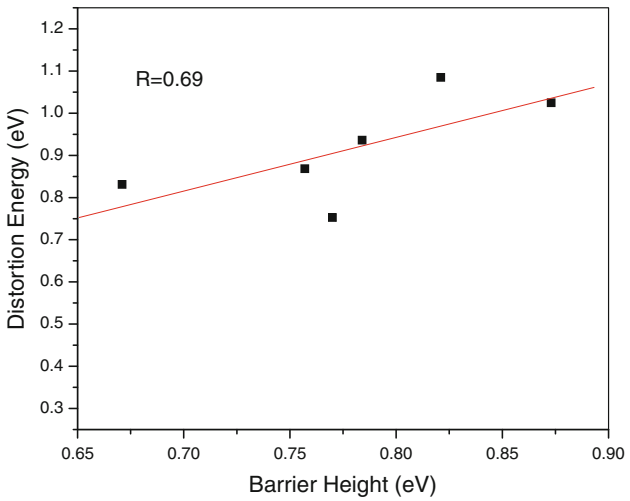

Fig. 4 Relationship between barrier heights (relative activation energy) and the total distortion energy

isosurfaces in each step of the reaction reinforce the change in the π-electron density during the reactions between [3]dendralene and C_{60}.

The MESP features and associated changes in the geometrical parameters reveal that there is sufficient reorganization of double bonds of C_{60} and [3]dendralene. Consequently, alteration in the electron delocalization takes place during various stages of addition and formation of TS to stabilize cyclic adducts in the DA reaction. These findings are in close agreement with the previous observation by Geerlings and coworkers [39, 40].

4.3 Distortion energy

It is interesting to observe from Table 3 (E_{dis} of dienophile) that C_{60} undergoes significant structural changes during the formation of TSs. The E_{dis} values of diene reveal that the geometrical variation of the [3]dendralene is extremely large. Therefore, the relationship between the geometrical distortion and thermodynamics (kinetic) parameters was probed. The linear relationships between these parameters are given in Fig. 4. The calculated correlation coefficient (R) is 0.69.

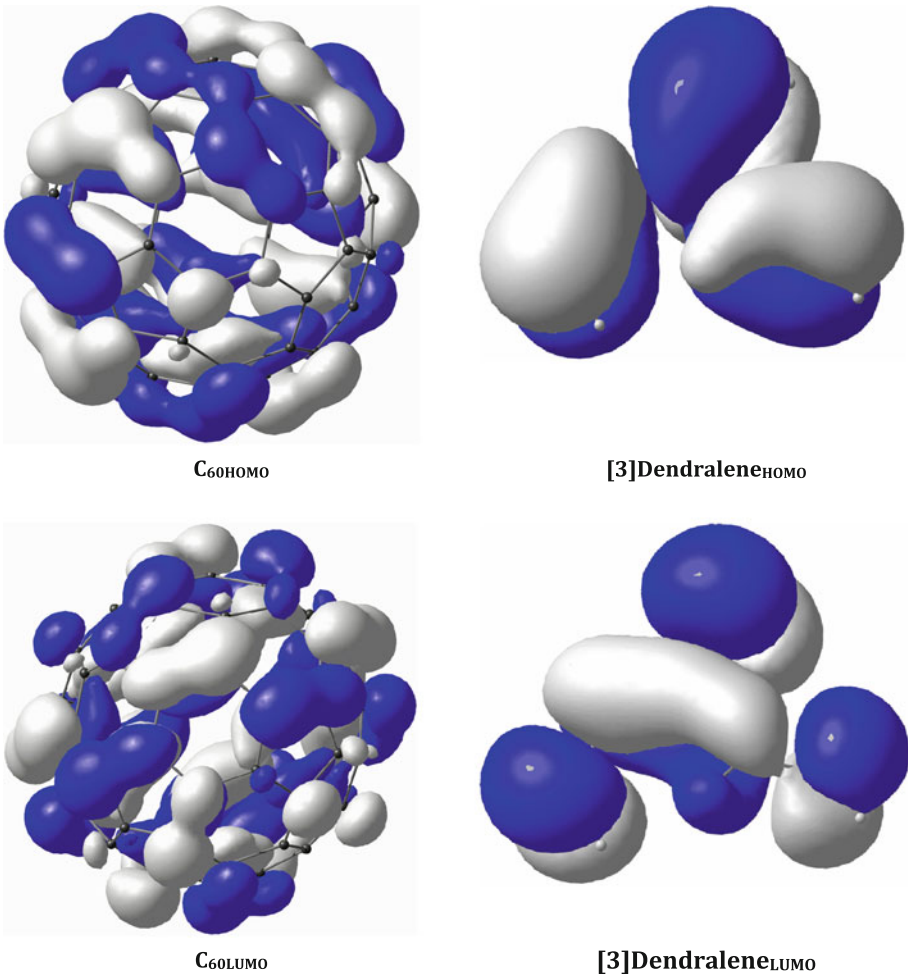

Fig. 5 Calculated molecular orbital isosurface of reactants (0.02 a.u)

4.4 Frontier molecular orbitals

The frontier molecular orbitals of starting diene and dienophile systems are displayed in Fig. 5 (All other are given in supplementary information). It can be observed from Fig. 5 that the HOMO of [3]dendralene exhibits two nodal planes along the σ_{2h} and σ_{2v} (molecular plane) planes, whereas corresponding LUMO shows three nodal planes including molecular one. It can be seen from the LUMO that two of the three nodal planes are perpendicular to the molecular plane. Further, It can be seen from the LUMO of C_{60} that one of the nodal plane is perpendicular to [6,6] bond (another nodal plane containing the [6,6] bond) which can interact favorably with the HOMO of diene. But the HOMO of the C_{60} lacks the nodal plane (excluding nodal plane containing the [6,6] bond) and hence it cannot interact with the diene. Therefore, the scrutiny of frontier molecular orbitals surfaces reveals that HOMO of [3]dendralene can favorably interact with the LUMO of C_{60} and thus the reactions are driven by normal electron demand. The calculated HOMO and LUMO gaps of various reactants are given in Table 4. These values reinforce the same findings.

Table 4 Normal ($\mathbf{1}^a$) and Inverse ($\mathbf{2}^b$) electron demands calculated using HOMO–LUMO energies of reactants

Adduct	$\mathbf{1}^a$ (eV)	$\mathbf{2}^b$ (eV)
1	2.870	5.120
1–1′	3.010	4.750
1–1′–2	3.142	4.527
1–1′–2–2′	3.443	4.352
1–1′–2–2′–3	3.538	4.171
1–1′–2–2′–3–3′	4.024	4.311
1–2	3.223	4.567
1–2–1′	3.670	4.615

$1^a = LUMO_{dienophile} - HOMO_{diene}$ of the reactants

$2^b = LUMO_{diene} - HOMO_{dienophile}$ of the reactants involved in the formation of the corresponding adducts

4.5 Energy decomposition analysis

The calculated various components of the interaction energy at TSs are presented in Table 5. The calculated sum of Pauli repulsion and electrostatic terms provides information on the steric interaction. It can be seen that the steric interaction is marginally high for the $\mathbf{TS_{1–1′–2–2′–3}}$ and $\mathbf{TS_{1–1′–2–2′–3–3′}}$ due to the addition of five and six [3]dendralenes. It is interesting to observe that minimum dispersion contribution is found in the case of $\mathbf{TS_1}$ which is about 66%. A maximum of 98% of dispersion contribution is observed in the stabilization of $\mathbf{TS_{1–1′–2–2′}}$. Overall findings reveal that dispersion interaction plays a significant role in the addition reaction between C_{60} and [3]dendralene.

4.6 Electronic properties of functionalized C_{60}

The calculated density of states for various adducts along with C_{60} are depicted in Fig. 6. The vertical red line represents the energy of Fermi level (E_f). The E_f values are calculated from the HOMO and LUMO energies at the same level of theory [66]. Results show that the E_f values increases linearly with the number of dendralenes and the electron density near the Fermi level is affected slightly. The calculated HOMO–LUMO gap (E_{gap}) of the various products is given in Table 6 along with that of C_{60}. The calculated values range from 1.42 to 1.98 eV. Examination of results reveals that changes in the E_{gap} values along reaction path **1**→**1–2**→**1–2–1′** are larger than that of **1**→**1–1′**→**1–1′–2**. Further, the calculated E_{gap} values demonstrates that the adducts **1**, **1–2**, **1–1′**, **1–1′–2**, **1–1′–2–2′** yield the smaller E_{gap} values than the parent C_{60}, whereas the other adducts shows the larger values. Thus the electronic properties of C_{60} are marginally influenced by the addition of [3]dendralene.

Table 5 The calculated various energy components of various transition states

TSs	V^{Pauli}	E^{Elec}	E^{Steric}	$E^{Orbital}$	$E^{Dispersion}$	BE
$\mathbf{TS_1}$	6.183	−3.129	3.054	−3.396	−0.651	−0.993
$\mathbf{TS_{1–1′}}$	6.032	−3.073	2.958	−3.270	−0.669	−0.981
$\mathbf{TS_{1–1′–2}}$	6.139	−3.102	3.037	−3.326	−0.669	−0.958
$\mathbf{TS_{1–1′–2–2′}}$	4.877	−2.553	2.324	−2.336	−0.715	−0.727
$\mathbf{TS_{1–1′–2–2′–3}}$	6.321	−3.172	3.149	−3.386	−0.670	−0.907
$\mathbf{TS_{1–1′–2–2′–3–3′}}$	6.866	−3.423	3.444	−3.693	−0.678	−0.928
$\mathbf{TS_{1–2}}$	6.045	−3.072	2.973	−3.294	−0.670	−0.990
$\mathbf{TS_{1–2–1′}}$	6.232	−3.142	3.090	−3.363	−0.659	−0.932

All the energies are given in eV

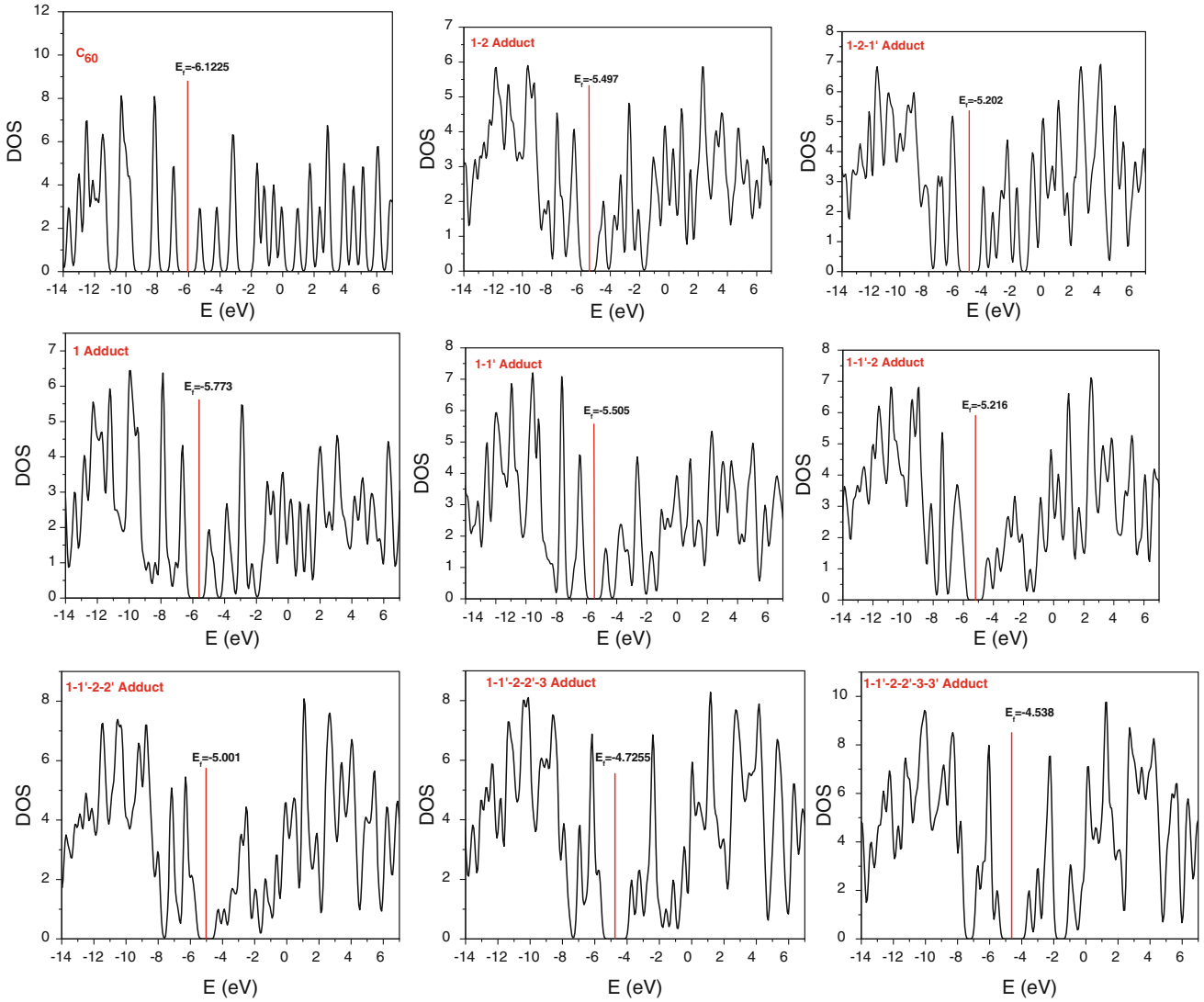

Fig. 6 Density of states (DOS) of the isolated C_{60} and various adducts

Table 6 Calculated HOMO–LUMO gaps (E_{gap}) of C_{60} and various adducts

System	E_{gap}
C_{60}	1.68
1	1.48
1–1′	1.42
1–1′–2	1.51
1–1′–2–2′	1.45
1–1′–2–2′–3	1.96
1–1′–2–2′–3–3′	1.98
1–2	1.50
1–2–1′	1.92

All the energies are in eV

5 Conclusions

It is found from the results that C_{60} can be functionalized by using [3]dendralene. The geometries of various TSs and products explicitly provide asynchronous nature of the product formation and the changes in the π-electron cloud of the C_{60}. Thermodynamic and kinetic parameters clearly demonstrate the feasibility of formation of one mono (**1**), two bis (**1–1′** and **1–2**), two tris (**1–1′–2** and **1–2–1′**), one tetrakis (**1–1′–2–2′**), one pentakis (**1–1′–2–2′–3**), and one hexakis (**1–1′–2–2′–3–3′**) adducts. Further, the bis adduct **1–2** formation is both thermodynamically as well as kinetically more feasible when compared with the **1–1′**. The geometrical distortion is quantified using distortion

energy which bears linear relationship with the reaction barrier. The frontier molecular orbitals study shows the normal electron demand of the DA addition of C_{60} with [3]dendralene. The energy decomposition analysis highlights that both the dispersion interaction and steric factors are responsible for the stabilization of TSs. The electronic properties of the functionalized C_{60} show that these properties are slightly influenced addition of [3]dendralene.

Acknowledgments The authors dedicate this paper to Prof. E. D. Jemiss on his 60th birthday. We thank the Center of Excellence for Computational Chemistry (Project No. NWP-53), Council of Scientific and Industrial Research (CSIR), New Delhi for financial support. One of the authors (P. R.) wishes to thank CSIR, New Delhi, India, for the award of Research Fellowship. We thank anonymous referees for their valuable suggestions and comments.

References

1. Trahanovsky S, Koeplinger KA (1992) J Org Chem 57:471
2. Bew SP, Sweeney JB (1994) Synthesis 698
3. Bew SP, Sweeney JB (1997) Synlett 1273
4. Cadogan JIG, Cradock S, Gillam S (1991) Chem Commun 114
5. Kohlman RS, Apstein AJ (1998) In handbook of conducting polymers, 2nd edn. Marcel Dekker, New York
6. Nalwa HS (1997) Handbook of organic conductive molecules and polymers. Wiley, Chichester
7. Hopf H (2000) Classics in hydrocarbon chemistry: syntheses, concepts, perspectives. Wiley–VCH, Weinheim, Germany
8. Hopf H (2001) Angew Chem Int Ed 40:705
9. Hopf H (1984) Angew Chem Int Ed 23:948
10. Alan DP, Anthony CW, Sherburn MS (2005) J Am Chem Soc 127:12188
11. Gomotsang B, Alan DP, Anthony CW, Sherburn MS (2008) Angew Chem Int Ed 47:910
12. Tanya AB, Alan DP, Anthony CW, Paddon-Row MN, Sherburn MS (2007) Org Lett 9:4861
13. Miller NA, Willis AC, Paddon-Row MN, Sherburn MS (2007) Angew Chem Int Ed 46:937
14. Hirsch A (1994) The chemistry of the fullerenes. George Thieme Verlag Stuttgart, New York
15. Diederich F, Thilgen C (1996) Science 271:317
16. Samal S, Sahoo SK (1997) Bull Mater Sci 20:141
17. Wei X, Wu MF, Qi L, Xu Z (1992) J Chem Soc Perkin Trans 2:1389
18. Richardson CF, Schuster DI, Wilson SR (2000) Org Lett 2:1011
19. Okamura H, Miyazono K, Minoda M, Komatsu K, Fukuda T, Miyamoto T (2000) J Polym Sci Part A Polym Chem 38:3578
20. Samal S, Geckeler KE (2000) Chem Commun 21:1101
21. Wharton T, Kini VU, Mortis RA, Wilson LJ (2001) Tetrahedron Lett 42:5159
22. Diederich F, Thilgen C (1996) Science 271:317
23. Lembo A, Tagliatesta P, Guldi DM, Wielopolski M, Nuccetelli M (2009) J Phys Chem A 113:1779
24. Diederich F, Jonas U, Gramlich V, Hermann A, Ringsdorf H, Thilgen C (1993) Helv Chim Acta 76:2445
25. Lamparth I, Maichle-Mossner C, Hirsch A (1995) Angew Chem Int Ed Engl 34:1607
26. Paquette LA, Trego WE (1996) Chem Commun 419
27. Herrera A, Martinez R, Gonzalez B, Illescas B, Martin N, Seoane C (1997) Tetrahedron Lett 38:4873
28. Torres-Garcia G, Luftmann H, Wolff C, Mattay J (1997) J Org Chem 62:2752
29. Tome AC, Enes RF, Cavaleiro JAS, Elguero J (1997) Tetrahedron Lett 38:2557
30. Nikos C, Michael O (2001) Org Lett 3:545
31. Krautler B, Maynollo J (1995) Angew Chem Int Ed 34:87
32. Krautler B, Miiller T, Maynollo J, Gruber K, Kratky C, Ochsenbein P, Schwarzenbach D, Burg HB (1996) Angew Chem Int Ed 35:1204
33. Lamparth I, Maichle-Mossmer C, Hirsch A (1995) Angew Chem Int Ed 34:1607
34. Hirsch A, Lamparth I, Karfunkel HR (1994) Angew Chem Int Ed 33:437
35. Hirsch A, Lamparth I, Grosser T (1994) J Am Chem Soc 116:9385
36. Meidine MF, Roers R, Langley GL, Avent AG, Darwish AD, Firth S, Kroto HW, Taylor R, Walton DRM (1993) Chem Commun 1342
37. Haddon RC, Brus LE, Raghavachari K (1986) Chem Phys Lett 125:459
38. Sola M, Mestres J, Marti J, Duran M (1994) Chem Phys Lett 231:325
39. Manoharan M, De Proft F, Geerlings P (2000) J Org Chem 65:6132
40. Amat MC, Lier GV, Sola M, Duran M, Geerlings P (2004) J Org Chem 69:2374
41. Mestres J, Sola M (1998) J Org Chem 63:7556
42. Cases M, Duran M, Mestres J, Martin N, Sola M (2001) J Org Chem 66:433
43. Mas-Torrent M, Rodriguez-Mias RA, Sola M, Molins MA, Pons M, Vidal-Gancedo J, Veciana J, Rovira C (2002) J Org Chem 67:566
44. Alvarez A, Ochoa E, Verdecia Y, Suarez M, Sola M, Martin N (2005) J Org Chem 70:3256
45. Illescas BM, Martin N, Poater J, Sola M, Aguado GP, Ortuno RM (2005) J Org Chem 70:6929
46. Izquierdo M, Osuna S, Filippone S, Martin-Domenech A, Sola M, Martin N (2009) J Org Chem 74:1480
47. Izquierdo M, Osuna S, Filippone S, Martin-Domenech A, Sola M, Martin N (2009) J Org Chem 74:6253
48. Delgado JL, Osuna S, Bouit PA, Martinez-Alvarez R, Espldora E, Sola M, Martin N (2009) J Org Chem 74:8174
49. Sola M, Duran M, Mestres J (1996) J Am Chem Soc 118:8920
50. Osuna S, Swart M, Sola M (2011) J Phys Chem A 115:3491
51. Dinadayalane TC, Vijaya R, Smitha A, Sastry GN (2002) J Phys Chem A 106:1627
52. Gerry AG, Ian HH, Andrew CM, Jonathan MP, Ricard R, Mark AV (2006) J Am Chem Soc 128:13130
53. Vildan G, Kelli SK, Andrew GL, Patrick SL, Michael DB, Houk KN (2003) J Phys Chem A 107:11445
54. Jayapal P, Sundararajan M, Rajaraman G, Venuvanalingam P, Kalagi K, Gadre SR (2008) J Phys Org Chem 21:146
55. Becke AD (1993) J Chem Phys 98:5648
56. Lee C, Yang W, Parr RG (1988) Phys Rev B 37:785
57. Grimme S (2006) J Chem Phys 124:034108
58. Schwabe T, Grimme S (2007) Phys Chem Chem Phys 9:3397
59. Frisch MJ, Trucks GW, Schlegel HB, Scuseria GE, Robb MA, Cheeseman JR, Montgomery JA Jr, Vreven T, Kudin KN, Burant JC, Millam JM, Iyengar SS, Tomasi J, Barone V, Mennucci B, Cossi M, Scalmani G, Rega N, Petersson GA, Nakatsuji H, Hada M, Ehara M, Toyota K, Fukuda R, Hasegawa J, Ishida M, Nakajima T, Honda Y, Kitao O, Nakai H, Klene M, Li X, Knox JE, Hratchian HP, Cross JB, Bakken V, Adamo C, Jaramillo J, Gomperts R, Stratmann RE, Yazyev O, Austin AJ, Cammi R, Pomelli C, Ochterski JW, Ayala PY, Morokuma K, Voth GA, Salvador P, Dannenberg JJ, Zakrzewski VG, Dapprich S, Daniels

AD, Strain MC, Farkas O, Malick DK, Rabuck AD, Raghavachari K, Foresman JB, Ortiz JV, Cui Q, Baboul AG, Clifford S, Cioslowski J, Stefanov BB, Liu G, Liashenko A, Piskorz P, Komaromi I, Martin RL, Fox DJ, Keith T, Al–Laham MA, Peng CY, Nanayakkara A, Challacombe M, Gill PMW, Johnson B, Chen W, Wong MW, Gonzalez C, Pople JA (2004) Gaussian 03 revision E.01 Gaussian Inc: Wallingford CT

60. Amsterdam Density Functional (ADF) version 2009.01. http://www.scm.com
61. Morokuma K, Kitaura K (1981) Energy decomposition analysis of molecular iteractions: in chemical applications of atomic and molecular electrostatic potentials. Plenum, New York
62. Ziegler T, Rauk A (1977) Theor Chim Acta 46:1
63. Ziegler T, Rauk A (1979) Inorg Chem 18:1558
64. Bickelhaupt FM, Baerends EJ (2000) In reviews in computational chemistry. Wiley, New York
65. Jemmis ED, Subramanian G, Sastry GN, Mehta G, Shirsat RN, Gadre SR (1996) J Chem Soc Perkin Trans 2:2343
66. Malolepsza E, Witek HA, Irle S (2007) J Phys Chem A 111:6649